Lift Enhancement on Unconventional Airfoils

W.W.H. Yeung
School of Mechanical and Aerospace Engineering
Nanyang Technological University, North Spine (N3), Level 2
50 Nanyang Avenue, Singapore 639798
mwhyeung@ntu.edu.sg

Abstract: Lift augmentation on airfoils is a critical task to an aerodynamicist when asked to design new wings. Flow visualization studies on a corrugated airfoil confirm that the trapped vortices lead to a modification of the effective wing shape and an increase in lift. Considerable lift enhancement is found in the experimental measurements on a wing model incorporated with a backward-facing step on the upper surface because of a trapped vortex. Furthermore, a leading-edge rotating cylinder (which behaves like a vortex) effectively extend the lift curve of an airfoil without substantially affecting its slope, thus increasing the maximum lift and delaying stall. While theoretical studies of vortex trapping are limited to airfoils with smooth surfaces, this paper explores the ability of trapping single and multiple vortices on airfoils with surface discontinuities, such as cavities, corrugations, or a rotating cylinder. Streamlines, surface pressure distributions and the vortex trajectories are presented in the hope to advance the knowledge on lift enhancement for flow past unconventional airfoils.

1. Introduction

An airfoil section, which is the essential part of a wing, has its primary task as a lift generator. The proper functioning of the airfoil is the prerequisite to the satisfactory performance of the lifting surface. An aerodynamicist is often faced with the challenge of optimizing and enhancing its lift without seriously increasing the drag. Over the years, many different methods of enhancing the lift have been proposed, verified by wind-tunnel tests and eventually realized. Typical examples include (a) the multi-element high-lift configuration of the Boeing 727 wing section consisting of a leading-edge slat, Krueger leading-edge flap and triple-slotted flaps in Fig. 1a from [1], (b) the Custer Channel Wing aircraft tested by NACA from [2] and (c) the rotating cylinders at the wing-flap junctions of an OV-10A at NASA-Ames [3].

(a) Boeing 727 wing section (b) Custer Channel Wing (c) OV-10A

Fig.1 Examples of high-lift devices

From examining a typical lift curve and the corresponding nature of flow over an airfoil in Fig. 2 from [4], the loss of lift at high angles of attack is closely associated with flow separation over the suction surface of the airfoil. Therefore, it is traditionally believed that maintaining attached flow there is critical in lift generation.

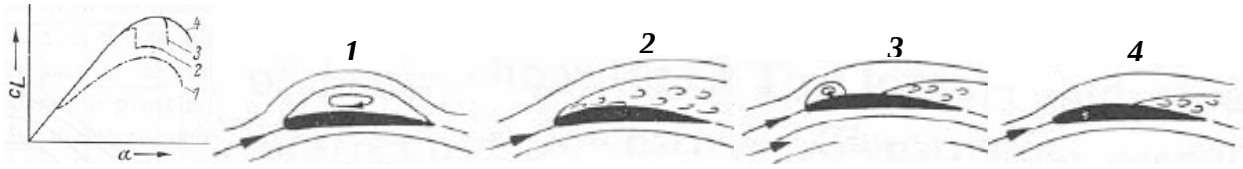

Fig. 2 Lift curve variations and nature of flow from [4].

The vortical flow induced by leading-edge separation over the delta wing in Fig. 3a & b from [5] has been found beneficial to generating lift. The consequence of this vortical flow, as depicted in Fig. 3c from [6], is the production of two large suction peaks due to the high-speed flow induced by these vortices.

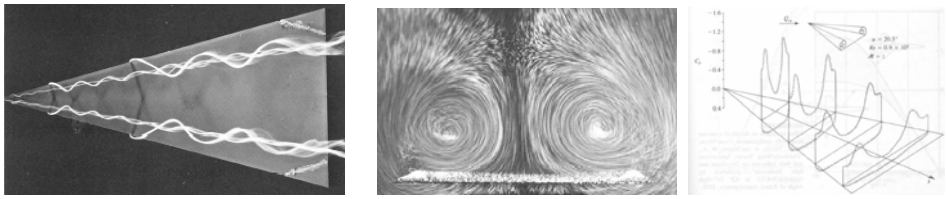

(a) top view (b) cross section (c) pressure distribution

Fig. 3 Vortical flow and surface pressure distributions of a delta wing from [5, 6].

Flow visualization studies in [7] on a corrugated airfoil confirm that vortices are trapped on the airfoil (see Fig. 4) and they lead to a modification of the effective wing shape and an increase in lift. Considerable lift enhancement is found in the experimental measurements in [8] on a wing model in Fig. 5 incorporated with a backward-facing step on the upper surface because of a trapped vortex. As reported in [9], a leading-edge rotating cylinder (which behaves like a stationary vortex) in Fig. 6 effectively extend the lift curve of an airfoil without affecting its slope, thus increasing the maximum lift and delaying stall.

(a) profile (b) trapped vortices

Fig. 4 Corrugated airfoil from [7].

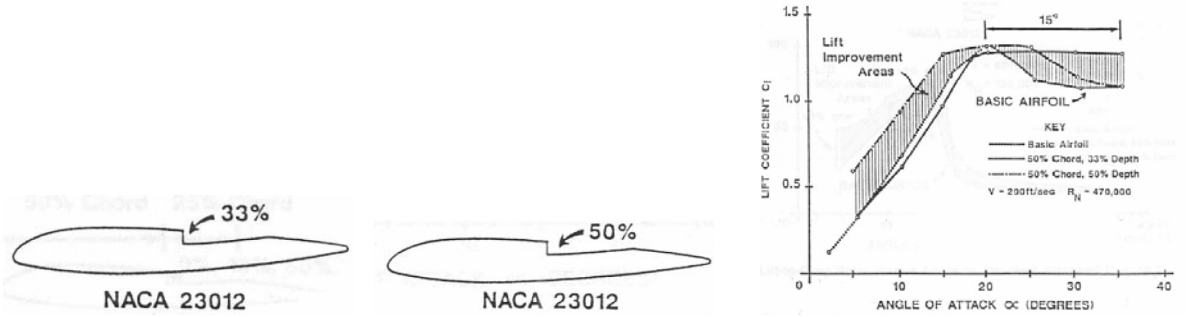

(a) 33% step (b) 50% step (c) lift vs. angle of attack

Fig. 5 Airfoils with backward-facing steps from [8].

(a) cylinder speed $= 0$ (b) cylinder speed $= 4$ times freestream speed

Fig. 6 Airfoil with leading-edge rotating cylinder from [9].

As reported by Huang and Chow [10], a free vortex may be theoretically captured by a Joukowsky airfoil at certain neighboring positions at which the vortex becomes stationary. The increase in lift can be as high as 200%. Their linear analysis reveals that all equilibrium positions are unstable, except those in a small region near the trailing edge of the airfoil. When the vortex is displaced by a finite, instead of an infinitesimal, distance from the equilibrium position, the vortex always goes away from its equilibrium position [11]. Therefore, the stable equilibrium positions as predicted by the linear theory are all unstable, if the perturbation amplitudes are not small. This paper presents a theoretical study on vortex trapping over an unconventional airfoil which has cavities, corrugations or a rotating cylinder. Calculations show that such a geometrical modification allows not only a single but multiple vortices to be trapped. Suction peaks have been found on the airfoil surface, resulting in lift enhancement.

2. Single cavity

Consider uniform flow U past a two-dimensional cavity in the physical plane $z = x + iy$, as shown in Fig. 7a. The presence of sharp edges causes the flow to separate at point A and reattach at point B such that inside the cavity the flow is expected to vortical in nature. In the context of inviscid and incompressible, the complex potential containing a single vortex of strength Γ (i.e. the simplest case) inside the cavity may be written as

$$F(\zeta) = U\zeta + \frac{i\Gamma}{2\pi}\log\left(\frac{\zeta-\zeta_v}{\zeta-\overline{\zeta}_v}\right) \qquad \ldots(1)$$

where

$$\zeta = \frac{2Ui}{n}\cot\left(\frac{2}{n}\tan^{-1}\left(\frac{i}{z}\right)\right) \qquad \ldots(2)$$

It is noted here that ζ_v represents the location of the vortex in terms of variable ζ, and $\overline{\zeta}_v$ is its complex conjugate. n, which is a real number, determines the depth of the cavity. In particular, when $n=3$, a semi-circular cavity is formed. The strength and location of the vortex are determined by satisfying the following conditions:

a) $\dfrac{dF}{d\zeta} = 0$ at points A and B such that a streamline joining points A and B is created,

b) $\dfrac{dF/d\zeta}{dz/d\zeta} - \dfrac{i\Gamma}{2\pi}\dfrac{1}{z-z_v} = 0$ at $\zeta = \zeta_v$ (i.e. $z = z_v$) such that the vortex is stationary in physical plane z.

The mean pressure p along the cavity boundary may be computed by using the Bernoulli's equation. When normalized by the undistributed pressure p_∞ and the dynamic pressure $\rho U^2/2$, the usual pressure coefficient $c_p = 2(p-p_\infty)/(\rho U^2)$ results. Based on the Lagrangian description, the trajectory of the vortex, when given a initial finite displacement from the equilibrium point, is found by integrating the equations of motion

$$\frac{dx}{dt} = \mathrm{Re}\left(\frac{dF/d\zeta}{dz/d\zeta}\right), \qquad -\frac{dy}{dt} = \mathrm{Im}\left(\frac{dF/d\zeta}{dz/d\zeta}\right) \qquad \ldots(3)$$

The steady flow pattern, the mean pressure distribution and a typical plot of the vortex trajectory are given in Fig. 7. It is noted that the inner streamline in Fig. 7a is generally different from the vortex trajectory in Fig. 7c, even though they share a common point marked by the cross. Also shown in Fig. 7c is that the vortex returns to that position after being displaced by a finite distance away from it. The equilibrium position of the captured vortex is considered to be stable.

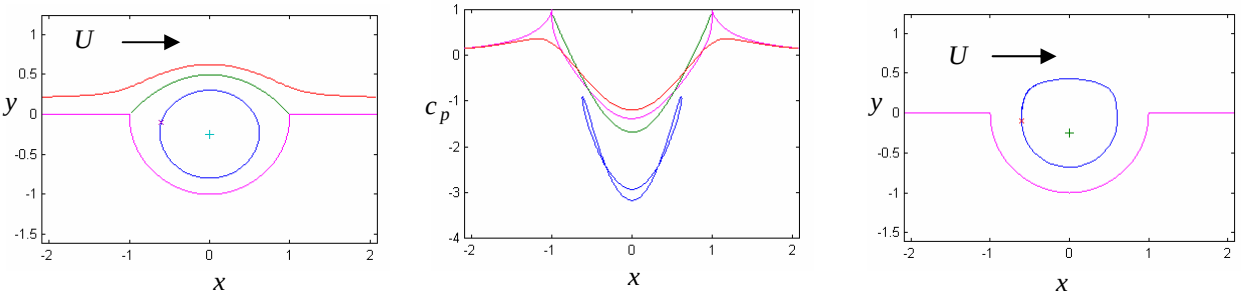

(a) steady flow pattern (b) pressure variation (c) vortex trajectory

Fig. 7 Flow past a semi-circular cavity.

Using a conformal mapping sequence, such a cavity can be incorporated on to a Joukowsky airfoil of chord c, as depicted in Fig. 8a. A high suction peak is induced by the standing vortex on the upper surface of the airfoil, as depicted in Fig. 8b. An enlarged view of the vortex trajectory in Fig. 8c indicates that the equilibrium point inside the cavity is stable.

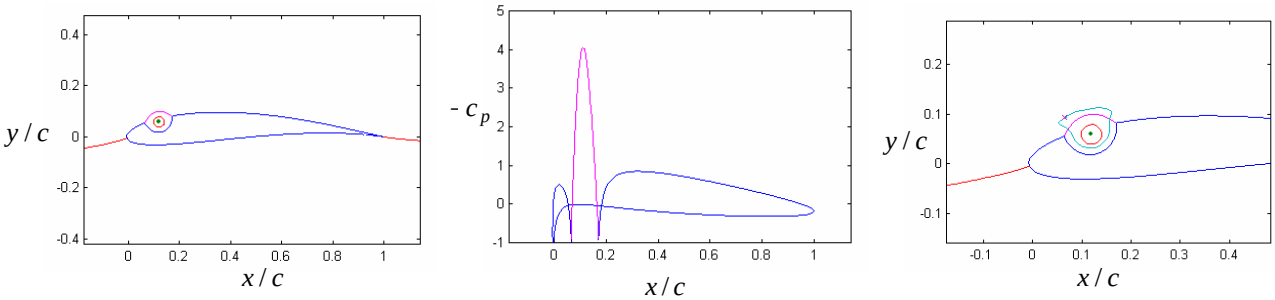

(a) steady flow pattern (b) pressure variation (c) vortex trajectory

Fig. 8 Flow past an airfoil with a semi-circular cavity

3. Corrugation

A single corrugation may be generated on a surface in the physical plane $z = x + iy$, as shown in Fig. 9a, from a flat horizontal boundary from the complex plane ζ by using

$$2\zeta = (z+\lambda)+(z+\lambda)^{1/2}(z-3\lambda)^{1/2} \qquad \ldots(4)$$

where λ is a complex number. Successive applications of (4) lead to double and triple corrugations in Fig. 9b and 9c, respectively. If N is the number of vortices involved, then in the presence of a uniform flow (1) is generalized to

$$F(\zeta) = U\zeta + \sum_{j=1}^{N} \frac{i\Gamma_j}{2\pi} \log\left(\frac{\zeta-\zeta_{vj}}{\zeta-\bar{\zeta}_{vj}}\right) \qquad \ldots(5)$$

where vortex of strength Γ_j is located at ζ_{vj}. The streamlines in Fig. 9 correspond to satisfying (a) flow separation at each sharp edge and (b) the condition of vanishing velocity at the vortex core. The trajectories are obtained by integrating the velocity components. Fig. 9 also depicts that each vortex is found to return to its original position around the equilibrium, when given a finite displacement. The pressure distributions in Fig. 10 are obtained when single, double and triple corrugations are incorporated onto an airfoil. In each case, the equilibrium is found to be stable.

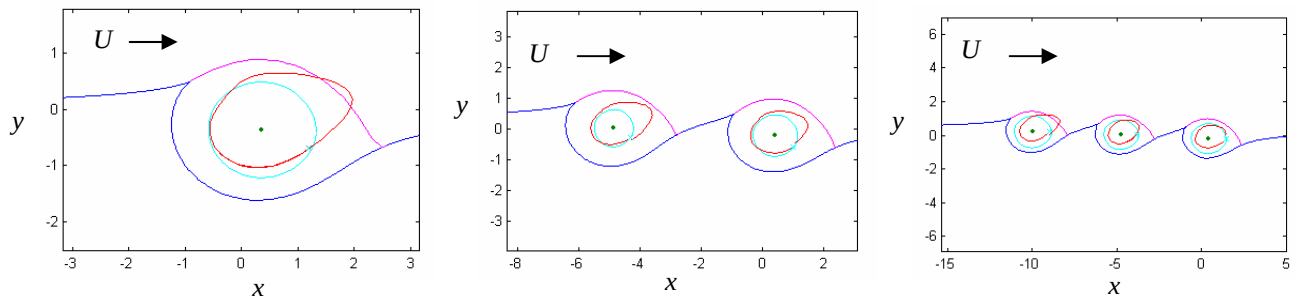

(a) single corrugation (b) double corrugations (c) triple corrugations

Fig. 9 Streamlines and vortex trajectories on corrugated surfaces.

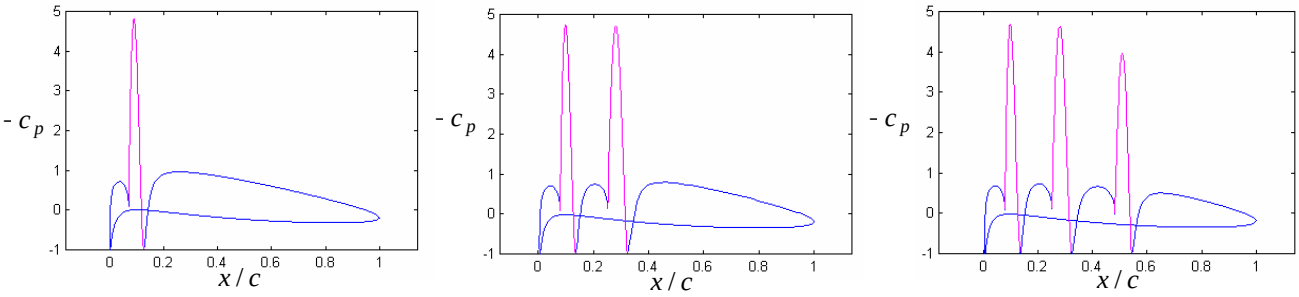

(a) single corrugation (b) double corrugations (c) triple corrugations

Fig. 10 Pressure distributions on corrugated airfoils

4. Airfoil with rotating cylinder

Equation (4), when combined with the method developed in Yeung and Parkinson [12], can be used to study the flow past an airfoil and a cylinder. An example is given in Fig. 11where the mean streamline pattern and the pressure distribution are shown.

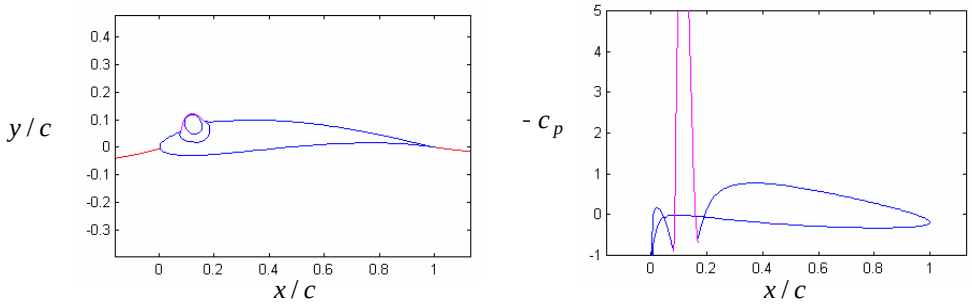

(a) streamline pattern (b) pressure distribution

Fig. 11 Flow model for airfoil with cylinder

5. Conclusion

In this study, a few theoretical models of unconventional airfoils are presented. The one having the highest lift is that of the triple corrugations, achieving a 10% more than that of a Joukowsky airfoil having the same thickness, camber and angle of attack. The presence of the standing vortices is the cause of the lift enhancement.

References

[1] Bertin, J. J. and Smith, M. *Aerodynamics for Engineers*, Prentice-Hall, 2nd edition.
[2] Blick, E. F. and Homer, V. *Journal of Aircraft*, Vol. 8, No. 4, pp. 234-238, 1971.
[3] http://turbulence.ucsd.edu/talks/aps02/tom.pdf
[4] Young, A.D. and Squire, H.B. *ARC RM* 2609, 1942/1951.
[5] Werle, H. *Houille Blanche*, Vol. 18, pp. 587-595, 1963.
[6] Hummel, D. AGARD CP-247, 1978.
[7] Buckholtz, R.H. *Journal of Fluids Engineering*, ASME, Vol. 108, pp. 93-97, 1984.
[8] Fertis, D.G. *Journal of Aerospace Engineering*, ASCE, Vol. 7, No. 3, pp. 328-339, 1994.
[9] Modi, V.J., Mokhtarian, F., Fernando, M.S.U.K. and Yokomizo T. *J. Aircraft*, Vol. 28, No. 2, pp. 104-112, 1991.
[10] Huang, M.K. and Chow C.Y. *AIAA Journal*, Vol. 20, No. 3, pp. 292-298, 1982.
[11] Chow, C.Y., Huang, M.K. and Yan, C.Z. *AIAA Journal*, Vol. 21, No. 5, pp. 657-658, 1985.
[12] Yeung, W.W.H. and Parkinson, G.V. *Journal of Fluid Mechanics*, Vol. 251, pp. 203-218, 1993.